Archive of Applied Mechanics (2023) 93:2129–2144
https://doi.org/10.1007/s00419-023-02376-6

ORIGINAL

Huong Quoc Cao · **Ngoc-An Tran**

Multi-objective optimal design of double tuned mass dampers for structural vibration control

Received: 8 February 2022 / Accepted: 7 February 2023 / Published online: 14 March 2023

Abstract A double tuned mass damper (DTMD) for suppressing oscillations of civil structures is proposed in this study. DTMD is a combination of an undamped TMD and a smaller TMD. The impact of parameters on the essential characteristics, as well as the vibration absorption capacity of DTMD, is investigated. Using genetic algorithms (GA), the optimum parameters of DTMD are determined by minimizing the peak dynamic magnification factor of structural responses for a wide range of excitation frequencies. The effectiveness and robustness of DTMD are also compared with those of the optimized TMD having a similar weight as the DTMD. Furthermore, multi-objective optimization designs of DTMD (for both two-objective and three-objective) are also developed here. This study indicates that the DTMD is more effective than a single TMD. If keeping a similar efficiency to that of an optimized TMD, the optimum DTMD has a broader domain for choosing the frequency and damping ratio. In this sense, a DTMD is much more robust than a single TMD.

Keywords Double tuned mass damper · Tuned mass damper · Vibration control · Passive damper · Genetic algorithms · Multi-objective optimization

1 Introduction

The high demand for living spaces and offices in most big cities around the world [1, 1] in the past decades has led to a large number of high-rise buildings and office towers built. On the other hand, advances in the new material field and construction technology helped civil works recently constructed to be taller and lighter [1, 1]. However, they become more sensitive to external loadings such as earthquakes and extreme winds [1]. For this reason, the safety of building structures, as well as the comfort of occupants, is always a vital engineering issue [2]. Thus, it is essential to find a suitable and effective solution for reducing the dynamic responses of buildings, especially for super-tall towers.

Many solutions have been proposed and applied to mitigate structural responses. In the civil engineering field, adding damping devices to structures is one of the most common technologies adopted to reduce structural oscillations [1, 1]. In this approach, the tuned mass damper (TMD) is one of the most popular types. Many high-rise buildings in the world have been equipped with one or some TMDs and confirmed to significantly suppress oscillations such as the Sydney Tower, Citigroup Center skyscraper in New York, Taipei 101 skyscraper, Crystal

H. Q. Cao (✉)
School of Mechanical and Mechatronic Engineering, Faculty of Engineering and Information Technology, University of Technology Sydney, Sydney, NSW, Australia
e-mail: huong.q.cao@student.uts.edu.au

N.-A. Tran
Faculty of Mechanical Engineering and Mechatronics, PHENIKAA University, Hanoi, Vietnam

N.-A. Tran
A&A Green Phoenix Group JSC, PHENIKAA Research and Technology Institute (PRATI), Hanoi, Vietnam

Tower Building in Japan or Berlin Television Tower [4–6]. Although TMDs are passive vibration control devices, they have been proven to be simple and effective dampers [1, 4, 6–11] Furthermore, a TMD does not need a well-designed control algorithm and an external energy source [3, 3, 7, 12, 13]. Thus, using TMDs for reducing undesired vibrations is still a suitable strategy, and this strategy has also attracted attention from researchers. To enhance the performance and robustness of TMD, researchers have proposed and developed various modified types of TMD. For instance, Ikago et al. [14] introduced a tuned viscous mass damper (VMD) as a new seismic control device. A hybrid damping system was also developed by Jafarabad et al. [15]. This system was composed of a tuned mass damper (TMD) fixed on a friction damper device (FDD) to reduce the seismic vibrations of structures. Cao [3] proposed a hybrid vibration absorber composed of a tuned liquid column damper (TLCD) fixed on an undamped TMD. In these research works, obtained results have shown that improved TMD systems are superior to the traditional ones.

On the other hand, magnetorheological elastomers (MREs) have also been studied and applied in mitigating structural vibrations. To some extent, MREs can be considered as a solid form of magnetorheological fluid (MRF). Hence, they can change their stiffness or elastic modulus if the magnetic field changes and then instantly revert to their initial status once the magnetic field is removed. Due to this smart characteristic of MREs, MREs have been utilized to develop smart devices such as MRE isolators [16] or MRE absorbers [17, 17]. In particular, Zhu and Rui [17] proposed a semi-active vibration control system consisting of a magnetorheological elastomer (MRE) and a magnetorheological damper (MRD). The experimental results showed that the performance of the proposed system is significantly higher than that of the system only using the MRD. Sun et al. [18] introduced a magnetorheological elastomers-based tuned mass damper (MRE-TMD) to protect buildings from earthquakes. The innovation of this damper was based on the multi-layered MRE structure developed by Yang et al. [16]. Both the experimental and simulation results of the research showed the superiority of semi-active MRE-TMD over passive TMDs. Although using an MRE-TMD for structural response suppression is a potential approach, such an MRE-TMD still needs an external current supply source. Additionally, smart materials such as MREs are usually challenging to manufacture, and therefore, developing an MRE-TMD is quite expensive.

Equipping a double tuned mass damper (DTMD) on high-rise buildings to suppress structural vibrations induced by external forces is presented in this paper. Here, the proposed DTMD consists of an undamped TMD (denoted as TMD1) and a smaller regular TMD (denoted as TMD2) as Fig. 1. This DTMD model differs from DTMD models in previous research groups such as Li et al. [19] and Shen et al. [20]. In the works of Li et al. [19] and Shen et al. [20], DTMD models were composed of two regular TMDs. On the other hand, in our previous research work, a DTMD (consisting of two regular TMDs) used to reduce the structural responses has been developed (unpublished). The results from that research showed that the DTMD reaches maximum effectiveness if the damping ratio of larger TMD approaches zero. As a coincidence, this is also in accordance with the conclusions in the paper of Li et al. [19]. Unlike multiple tuned mass dampers (MTMD), a DTMD with an undamped primary TMD is remarkable convenient for the maintenance and installing process because of its simple configuration. Thus, these are reasons why a larger TMD undamped is used in the DTMD model of this study.

The paper is organized as follows. After the introduction, Sect. 2 shows an analysis model of the system coupled with a DTMD. Section 3 presents the parametric study of a DTMD for absorbing harmonically forced vibrations through numerical examples. In the next section, the optimal parameters of DTMD are also determined by solving its optimization problems. Genetic algorithms, one of the most powerful optimization algorithms, are utilized in this study. Then, the effectiveness and robustness of the optimum DTMD are compared with those of an optimized TMD that has the same weight as the DTMD. Furthermore, multi-objective optimal designs (for both two and three objectives) of DTMD are also developed and discussed in Sect. 5. Finally, conclusions drawn from this study are presented in Sect. 6.

2 Modeling of the DTMD-structure system

According to Gao et al. [10], natural frequencies of civil structures are normally separate. In this investigation, the DTMD is considered for mitigating a specific vibration mode of a multi-degree of freedom (MDOF) structure. Hence, the primary structure can be simplified as a single degree of freedom (SDOF) system, but the frequency of the SDOF system must be equal to the frequency of the mode controlled. The calculation model of the SDOF structure with a DTMD subjected to an external force is shown in Fig. 1, in which the DTMD is composed of an undamped TMD1 and a TMD2.

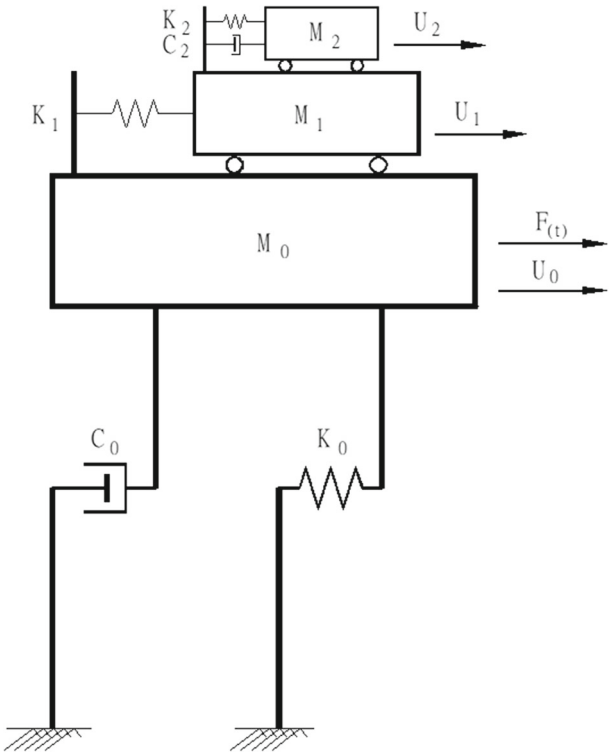

Fig. 1 Analysis model of the DTMD-structure system

2.1 Equations of motion

The equations of motion of the DTMD-structure system can be expressed as follows:

$$M_2\ddot{U}_2 + C_2\dot{U}_2 + K_2U_2 = -M_2(\ddot{U}_0 + \ddot{U}_1) \tag{1}$$

$$M_1\ddot{U}_1 + K_1U_1 - C_2\dot{U}_2 - K_2U_2 = -M_1\ddot{U}_0 \tag{2}$$

$$M_0\ddot{U}_0 + C_0\dot{U}_0 + K_0U_0 - K_1U_1 = F_{(t)} \tag{3}$$

In Eqs. (1), (2) and (3), U_0 is the absolute displacement of the structure, while U_1 and U_2 are the relative displacements of the TMD1 mass and the TMD2 mass, respectively. This means that the absolution displacement of the TMD1 mass is $U_1^{\text{absolute}} = U_1 + U_0$ and the absolution displacement of the TMD2 mass is $U_2^{\text{absolute}} = U_2 + U_1^{\text{absolute}} = U_2 + U_1 + U_0$. The structure has the generalized stiffness (K_0), damping coefficient (C_0), and mass (M_0). The mass and the stiffness of TMD1 are, respectively, M_1 and K_1. The parameters of TMD2 include the mass M_2, the stiffness K_2, and the damping C_2. Here, $F_{(t)}$ is the external force acting on the structure, which is considered as a harmonic force with the frequency Ω. The intensity of loading (F_0) is expressed by a nondimensional ratio Δ corresponding to the percentage of structural weight, as Gao et al. [10]:

$$F_{(t)} = F_0 sin(\Omega t) = \Delta M_0 g sin(\Omega t) \tag{4}$$

In Eq. (4), Δ is the external force intensity factor and g is the acceleration of gravity. In addition, for the sake of simplicity and convenience, let us introduce the following quantities:

The natural frequency of the TMD1

$$\omega_1 = \sqrt{\frac{K_1}{M_1}} \tag{5}$$

The natural frequency of the TMD2

$$\omega_2 = \sqrt{\frac{K_2}{M_2}} \tag{6a}$$

The damping ratio of the TMD2

$$\xi_2 = \frac{C_2}{2M_2\omega_2} \tag{6b}$$

The natural frequency of the primary structure

$$\omega_0 = \sqrt{\frac{K_0}{M_0}} \tag{7a}$$

The damping ratio of the primary structure

$$\xi_0 = \frac{C_0}{2M_0\omega_0} \tag{7b}$$

By combining Eqs. (1–4), the equations of motion governing DTMD-structure system can be written in matrix form:

$$\mathbf{M}\ddot{\mathbf{U}} + \mathbf{C}\dot{\mathbf{U}} + \mathbf{K}\mathbf{U} = \mathbf{F} \tag{8}$$

in which

$$\mathbf{M} = \begin{bmatrix} M_0 & 0 & 0 \\ M_1 & M_1 & 0 \\ M_2 & M_2 & M_2 \end{bmatrix} \tag{8a}$$

$$\mathbf{C} = \begin{bmatrix} C_0 & 0 & 0 \\ 0 & 0 & -C_2 \\ 0 & 0 & C_2 \end{bmatrix} \tag{8b}$$

$$\mathbf{K} = \begin{bmatrix} K_0 & -K_1 & 0 \\ 0 & K_1 & -K_2 \\ 0 & 0 & K_2 \end{bmatrix} \tag{8c}$$

$$\mathbf{F} = \begin{bmatrix} F_0 sin(\Omega t) \\ 0 \\ 0 \end{bmatrix} \tag{8d}$$

$$\mathbf{U} = \begin{bmatrix} U_0 \\ U_1 \\ U_2 \end{bmatrix} \tag{8e}$$

$$\dot{\mathbf{U}} = \begin{bmatrix} \dot{U}_0 \\ \dot{U}_1 \\ \dot{U}_2 \end{bmatrix} \tag{8f}$$

$$\ddot{\mathbf{U}} = \begin{bmatrix} \ddot{U}_0 \\ \ddot{U}_1 \\ \ddot{U}_2 \end{bmatrix} \tag{8g}$$

It is noted that the values of elements in matrices M, C, K of some papers [21, 22] differ from Eqs. (8a), (8b) and (8c). This is because U_0 is the absolute displacement of the structure, while U_1 and U_2 are the relative displacements of the TMD1 mass and the TMD2 mass, respectively (as previously mentioned in this paper). In the case of choosing U_0, U_1 and U_2, respectively, are the absolute displacements of the structure, the TMD1 mass and the TMD2 mass, then the values of terms in Eqs. (8a), (8b) and (8c) will be similar to those in the general formulas M, C, K of Khatibinia et al. [21] or Etedali and Rakhshani [22]. In this study, some nondimensional quantities are denoted as follows:

The mass ratio of the TMD1

$$\mu_1 = \frac{M_1}{M_0} \tag{9a}$$

The mass ratio of the TMD2

$$\mu_2 = \frac{M_2}{M_0} \tag{9b}$$

The mass ratio of the DTMD

$$\mu = \frac{M_1 + M_2}{M_0} = \mu_1 + \mu_2 \tag{9c}$$

In addition, the mass ratio between TMD1 and TMD2:

$$\mu_{21} = \frac{M_2}{M_1} = \frac{\mu_2}{\mu_1} \tag{9d}$$

Thus, Eq. (8) can be rewritten as follows:

$$\overline{\mathbf{M}}\ddot{\mathbf{U}} + \overline{\mathbf{C}}\dot{\mathbf{U}} + \overline{\mathbf{K}}\mathbf{U} = \overline{\mathbf{F}} \tag{10}$$

where

$$\overline{\mathbf{M}} = \begin{bmatrix} 1 & 0 & 0 \\ 1 & 1 & 0 \\ 1 & 1 & 1 \end{bmatrix} \tag{10a}$$

$$\overline{\mathbf{C}} = \begin{bmatrix} 2\xi_0\omega_0 & 0 & 0 \\ 0 & 0 & -2\mu_{21}\xi_2\omega_2 \\ 0 & 0 & 2\xi_2\omega_2 \end{bmatrix} \tag{10b}$$

$$\overline{\mathbf{K}} = \begin{bmatrix} \omega_0^2 & -\mu_1\omega_1^2 & 0 \\ 0 & \omega_1^2 & -\mu_{21}\omega_2^2 \\ 0 & 0 & \omega_2^2 \end{bmatrix} \tag{10c}$$

$$\overline{\mathbf{F}} = \begin{bmatrix} \Delta g sin(\Omega t) \\ 0 \\ 0 \end{bmatrix} \tag{10d}$$

$$\mathbf{U} = \begin{bmatrix} U_0 \\ U_1 \\ U_2 \end{bmatrix} \tag{10e}$$

$$\dot{\mathbf{U}} = \begin{bmatrix} \dot{U}_0 \\ \dot{U}_1 \\ \dot{U}_2 \end{bmatrix} \tag{10f}$$

$$\ddot{\mathbf{U}} = \begin{bmatrix} \ddot{U}_0 \\ \ddot{U}_1 \\ \ddot{U}_2 \end{bmatrix} \tag{10g}$$

Table 1 The first mode of the 76-story tower [24]

Parameter	Value
The natural frequency ω_0	1.0 rad/s
The damping ratio ξ_0	1%

2.2 Responses of the system DTMD-structure

The dynamic magnification factor (DMF) of the structural response in the steady state is given by [23]

$$\mathrm{DMF} = \frac{\mathrm{Max}U_0}{(F_0/K_0)} \tag{11}$$

Let us introduce the following dimensionless quantities.
The frequency ratio is

$$\alpha = \frac{\Omega}{\omega_0} \tag{12}$$

The tuning ratios (β_1, β_2) of TMD1 and TMD2, respectively, are denoted by

$$\begin{cases} \beta_1 = \frac{\omega_1}{\omega_0} \\ \beta_2 = \frac{\omega_2}{\omega_0} \end{cases}, \tag{13a}$$

and the tuning ratio of DTMD is set as

$$\beta_{12} = \frac{\omega_1}{\omega_2} = \frac{\beta_1}{\beta_2} \tag{13b}$$

Consequently, the structural response is a function of α, β_1, β_2, ξ_0, ξ_2, $\mu_1$andμ_2. Note that, the values of $\mu_1$andμ_2 can be computed through μ and μ_{21} from Eqs. (9c) and (9d). Apart from ξ_0 and α given by itself, the effects of β_1, β_2, ξ_2, $\mu_1$andμ_2 on the structural responses are investigated through parametric studies in the next section.

3 Parametric investigation

A parametric study involving the effects of the frequency range, mass ratios, and damping ratio on the effectiveness of DTMD is conducted through numerical examples. In the numerical model, the 76-story office tower in Melbourne, Australia, used in the paper of Varadarajan and Nagarajaiah [24], is applied to demonstrate the potential of installing a DTMD for vibration control. The first mode properties of the building are listed in Table 1. In addition, a range of excitation frequency corresponding to $0.5 \leq \alpha \leq 1.5$ is considered, and the external force is assumed by the intensity factor $\Delta = 0.003$.

3.1 Effects of the mass ratios $\boldsymbol{\mu}$, $\boldsymbol{\mu}_{21}$

With the mass ratio (μ) of 0.02, Fig. 2 describes the frequency response curve of the building for five different cases of μ_{21}. In the figure, the damping ratio ξ_2 of TMD2 is chosen to be 0.20, while the tuning ratios are assumed as $\beta_1 = \beta_2 = 1$. It can be seen in Fig. 2 that the DTMD is effective in controlling vibrations if the ratio of μ_{21} is chosen in (0, 1). In the case of $\mu_{21} = 0$, the DTMD becomes a single undamped TMD (TMD1). If the mass of TMD2 equal to the TMD1 mass ($\mu_{21} = 1$), the efficiency of DTMD is less significant. In this case, the structural response curve is similar to (but lower than) the curve of the system without DTMD. On the contrary, when the TMD2 mass is larger than the mass of TMD1 ($\mu_{21} > 1$), the control performance of DTMD is not significant. As observed in Fig. 2, a DTMD is no longer effective if the value of μ_{21} is large. In the case of $\mu_{21} = 10$, the structural response curve is most close to the response curve of the building without DTMD.

Figure 3 depicts the effect of the ratio μ_{21} on the peak dynamic magnification factor curve of the structure in a range of μ_{21} from 0 to 1. It is noted that the peak dynamic magnification factor (DMF_{max}) of the structural

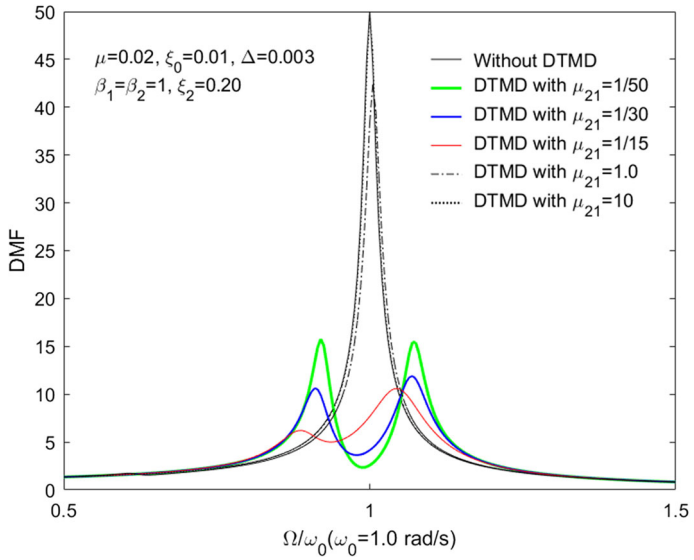

Fig. 2 The structural response curve for different values of μ_{21}

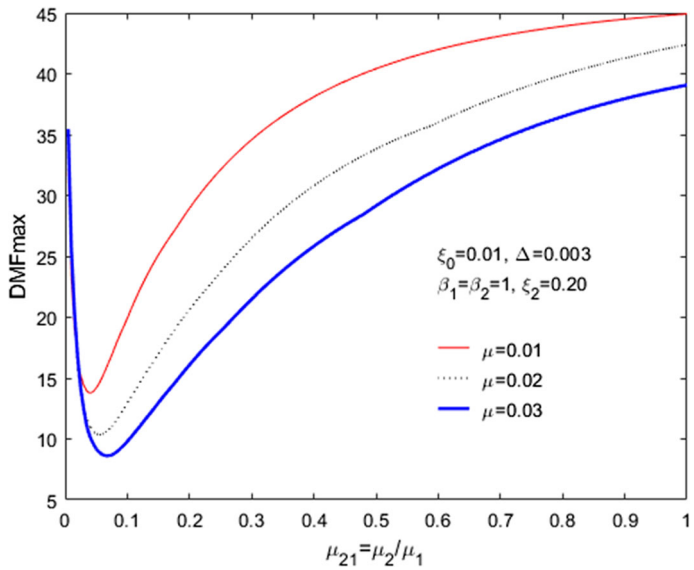

Fig. 3 The effect of μ_{21} on $\mathrm{DMF}_{\max}$ curve for different values of μ

response is defined by Eq. (15) in the wide frequency range corresponding to $0.5 \leq \alpha \leq 1.5$. As observed in Fig. 3, the minimum value of DMF_{max} decreases from 13.77 to 8.62 when μ increases from 1 to 3%. This means that the effectiveness of DTMD is improved significantly as μ rises. Furthermore, there exists an optimal value of μ_{21} corresponding to each given value of μ, and this optimum value also increases if the mass ratio μ increases. In the figure, the optimum value of μ_{21} is 0.04 at $\mu = 0.01$, while this value is 0.055 for $\mu = 0.02$ and 0.07 for $\mu = 0.03$.

3.2 Effects of the tuning ratios $\boldsymbol{\beta}_1$,$\boldsymbol{\beta}_2$, $\boldsymbol{\beta}_{12}$

The effect of the tuning ratio β_{12} on the DMF_{max} curve of the building response for five different values of β_1 is described in Fig. 4. In this investigation, the tuning ratio of DTMD (β_{12}) is considered in [0.5, 1.5], while the damping ratio of TMD2 (ξ_2) is 0.2, the value of $\mu = 0.02$ and the value of $\mu_{21} = 0.1$. Obviously, there is a nadir in each *DMFmax* curve. This means that there exists an optimum value of β_{12} corresponding to each

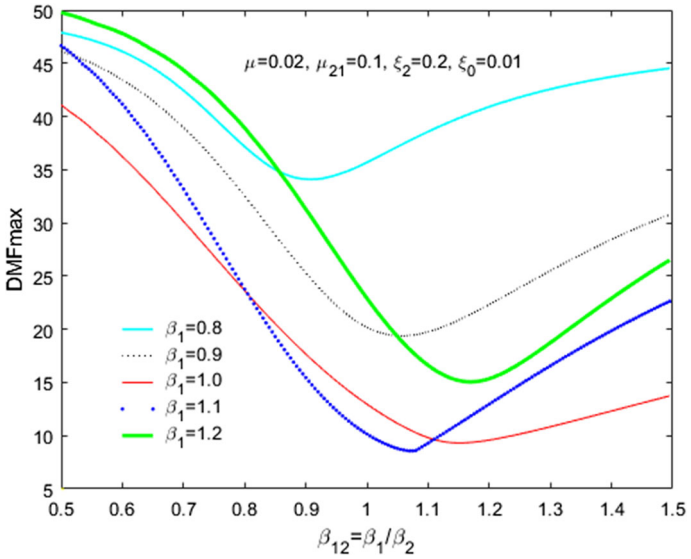

Fig. 4 The effect of β_{12} on $\mathrm{DMF}_{\max}$ curve with different values of β_1

value of β_1 given to minimize the value of *DMFmax*. The variation in this optimal value in the *DMFmax* curve is from 0.9 to 1.2 when the tuning ratio of TMD1 (β_1) changes within [0.8, 1.2]. Moreover, the effectiveness of DTMD is improved in the case that the value of β_1 increases from 0.8 to 1.1. In the figure, the lowest point value of *DMFmax* curve is 34.1 corresponding to $\beta_1 = 0.8$, and this value decreases to 8.613 in the case of $\beta_1 = 1.1$.

3.3 Effects of the damping ratio $\boldsymbol{\xi}_2$

Figure 5 presents the change of the DMF_{max} curve in five different cases of the damping ratio ξ_2, while the tuning ratio is chosen $\beta_2 = 1$ and the ratio μ_2/μ_1 is 1/10. In the calculation, the values of ξ_2, respectively, are 0.1, 0.2, 0.3, 0.4 and 0.5. It is observed in Fig. 5 that the lowest point value of the *DMFmax* curve decreases from 13.75 to 7.89 as ξ_2 increases from 0.1 to 0.3. However, this value is increased again (from 7.89 to 10.43) when ξ_2 changes from 0.3 to 0.5. In the figure, a smaller ξ_2 corresponds to the optimum value of β_1/β_2 that is larger. For instance, the optimal value obtained of β_{12} is 1.045 at $\xi_2 = 0.5$, but this value is 1.175 as the damping ratio ξ_2 decreases to 0.1.

Therefore, it can be concluded that (i) a DTMD is effective when the mass ratio of DTMD(μ_{21}) is in the range of (0, 1), and (ii) there exists a set of the optimum values of $\mu, \mu_{21}, \beta_1, \beta_2$ and ξ_2 to maximize the performance of a DTMD in mitigating the building vibrations.

4 Effectiveness and robustness of dtmd

4.1 Parametric optimization

The desired outcome of the parametric optimization is to minimize the value of DMF_{max} obtained by sweeping the range of excitation frequency which corresponds to the frequency ratio within $[\alpha_1, \alpha_2]$. The objective function of DMF_{max} can be given by

$$Obj = \{DMF_{\max} \rightarrow \boldsymbol{min}\} \tag{14}$$

here, the value of $DMF_{\max}$ is determined by Eq. (15), while α_1 and α_2 are the lower and upper limit of the frequency ratio. The variables of the objective function in Eq. (14) include the damping ratio, mass ratios and tuning ratios. It is, however, a challenge to obtain a closed-form solution for a set of optimum parameters of a DTMD. Therefore, using a powerful algorithm to search for the optimal or near-optimal solution for the above optimization problem is necessary. Nowadays, there are many techniques adopted for optimization problems

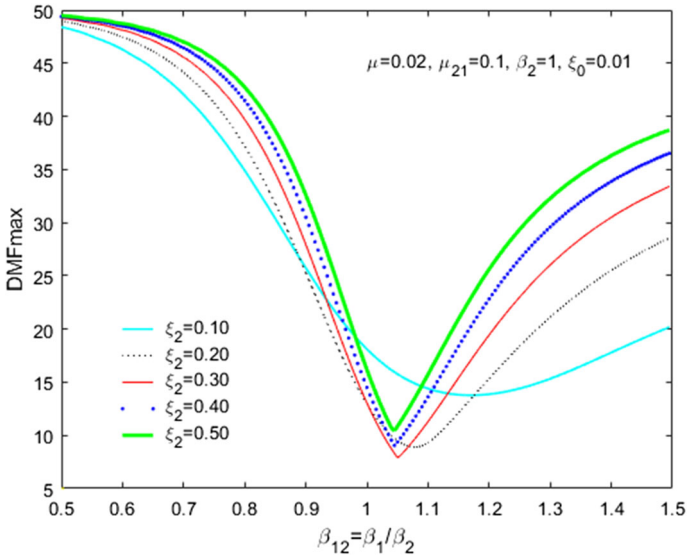

Fig. 5 The change of the DMF_{max} curve for different values of ξ_2

Table 2 Optimum parameters of DTMD

Symbol	β_1^{opt}	β_2^{opt}	μ^{fixed}	μ_{21}^{opt}	ξ_2^{opt}
Value	1.041	0.970	0.020	0.088	0.246

in many fields. However, genetic algorithms (GAs), an optimization technique based on a natural selection process, are well known as a potential optimization approach [25, 26]. Using GAs in the Optimization Tool of MATLAB, Table 2 reports the optimum parameters of DTMD obtained in the case of $\mu = 0.02$, while the optimal parameters of a single TMD with the same weight as the DTMD are $\xi_{\text{tmd}}^{\text{opt}}$=0.0883 and $\beta_{\text{tmd}}^{\text{opt}} = 0.9784$. Here, the input parameters of the building are taken from Table 1; the frequency ratio (α) is within [0.5, 1.5], and the ratio Δ is unchanged to be 0.003.

4.2 Comparisons between DTMD and TMD

(a) Performance index

The effectiveness of each damper in reducing the structural responses is evaluated through two of the major indices, which are the maximum dynamic magnification factor (DMF_{Max}) and the root-mean-square of the peak displacement response (RMS_{U_0}) of the building. It is also noted that the damper which gives the smaller value of DMF_{Max} or RMS_{U_0} is more effective. Here, the peak dynamic magnification factor (DMF_{Max}) of the structural response within the frequency range which corresponds to [α_1,α_2] is given by

$$\text{DMF}_{\text{Max}} = \text{Max}\{U_0\}_{\alpha_1}^{\alpha_2}/(F_0/K_0) \tag{15}$$

Furthermore, the root-mean-square (RMS) of the peak displacement response (e.g., Wu et al. [27]; Xue et al. [28]) can be computed by the following formula:

$$\text{RMS}_{U_o} = \sqrt{\frac{\sum_1^n (U_{0i})^2}{n}} \tag{16}$$

in which U_{0i} is the value of peak displacement response corresponding to α_i.

(b) Effectiveness of DTMD

Table 3 $\mathrm{DMF_{Max}}$ and RMS_{U_0} of each absorber

Configuration	$\mathrm{DMF_{Max}}$	RMS_{U_0}
Uncontrolled	50.00	0.264
Optimum TMD	8.567	0.126
Optimum DTMD	7.398	0.120

Table 3 reports evaluation indices of both of DTMD and TMD optimized in the case of $\mu = 0.02$. For the case of the uncontrolled building, $\mathrm{DMF_{Max}}$ and RMS_{U_0} of the structural response are, respectively, 50.0 and 0.264. As observed in Table 3, the values of $\mathrm{DMF_{Max}}$ and RMS_{U_0} of the building equipped with the DTMD are smaller than those of the system coupled with the TMD, respectively. Thus, it can be concluded that the effectiveness of the optimum DTMD is higher than that of TMD which has the same weight as the DTMD. In particular, with the same value of $\mu = 0.02$, the values of $\mathrm{DMF_{Max}}$ and RMS_{U_0} for the building with the optimized DTMD are 7.398 and 0.120, while these values of the system with the optimum TMD are 8.567 and 0.126, respectively. In this numerical example, the peak dynamic magnification factor of the structural response is reduced by 85.2% if the building is equipped with the DTMD optimized.

(c) Robustness of DTMD

It is, in fact, not easy to exactly measure the natural frequency of structures in the civil engineering area. Apart from the error in determining the natural frequency of structures (Yamaguchi and Harnpornchai [29]), there are different reasons leading to the change of the structural stiffness such as environment loadings or replaced components of the structure (Xue et al. [28]). As the structural stiffness (K_0) varies, the natural frequency (ω_0) and the damping ratio (ξ_0) of the structure also change. Therefore, to evaluate the robustness of a DTMD, a study on the impact of the drift in the structural stiffness is carried out in this section.

Figure 6 shows the robustness against the variation in the structural stiffness,ε_{K_0}, for both of the optimum DTMD and the single TMD optimized. In the figure, the drift of the building stiffness is considered in the range of [-30%, 30%]. It is also noted that the mass ratio $\mu = 0.02$ is unchanged in the calculation. As observed in Fig. 6, DTMD and TMD optimized have the largest effectiveness at the nominal stiffness $\varepsilon_{K_0} = 0\%$. This means the values of $\mathrm{DMF_{max}}$ of the building response in cases with the DTMD and with the TMD are 7.398 and 8.567, respectively (similar to the values of $\mathrm{DMF_{max}}$ in Table 3). Nevertheless, the DTMD and TMD optimized become non-optimized vibration absorbers because of the structural stiffness changes. In this sense, the performance of each damper is decreased. From Fig. 6, it can be concluded that the robustness of the DTMD is not better than that of the TMD for resisting the drift of the structural stiffness. However, if remaining the same level of efficiency as the optimized TMD, the DTMD offers a lot of options for the frequency and damping ratio to enhance the robustness of DTMD. This will be confirmed in the next section of multi-objective optimal designs of DTMD as well.

(d) Oscillations of the TMD1 and TMD2 in DTMD

In order to further understand how the DTMD vibrates, Fig. 7 shows the *DMF* curves of the TMD1 and TMD2 of the optimum DTMD. Moreover, Fig. 7 also includes the curves of the structure with and without the optimal DTMD. It is seen that the value of DMF_{max} in the uncontrolled system is 50.0, while this value of the system containing the DTMD is 7.398. For the TMD1 and TMD2 in the DTMD, they oscillate with large amplitudes. Although TMD2 is much smaller than TMD1 (μ_{21}=0.088, see Table 2), the maximum vibration amplitude of TMD2 is much larger than that of TMD1 (139.914 compared with 50.862). In other words, TMD2 plays a vital role in the DTMD, especially the damping coefficient of TMD2. Although the mass of TMD2 is much smaller than that of the optimized single TMD having the same weight as DTMD, the damping ratio TMD2 is much greater than that of the single TMD ($\xi_2^{opt} = 0.246$ in Table 2 compared with $\xi_{tmd}^{opt} = 0.0883$). In addition, to have a clearer look at the vibration amplitude and phase of the DTMD-structure system, the natural frequencies of the system and the mode shapes corresponding to these frequencies are depicted in Fig. 8. In this calculation, the natural frequencies of the system obtained are 0.85295, 1.0022 and 1.1813 rad/s. The mode shapes displayed in Fig. 8 also confirm that the oscillation of the TMD2 is the largest in all modes.

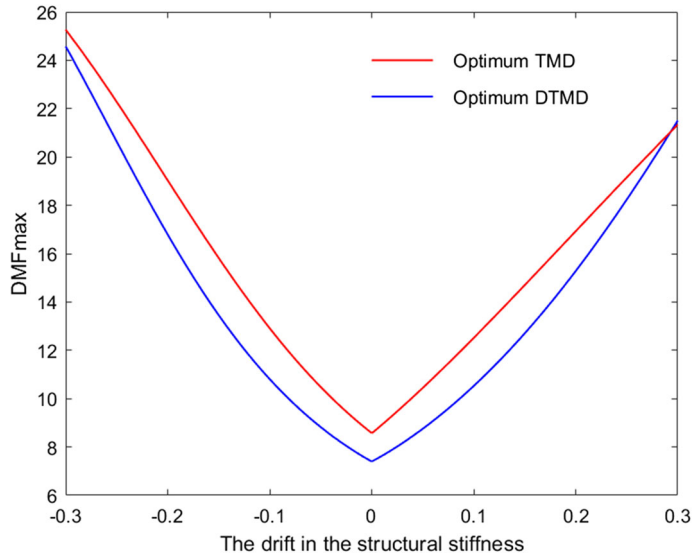

Fig. 6 The robustness against the change of K_0 of DTMD and TMD

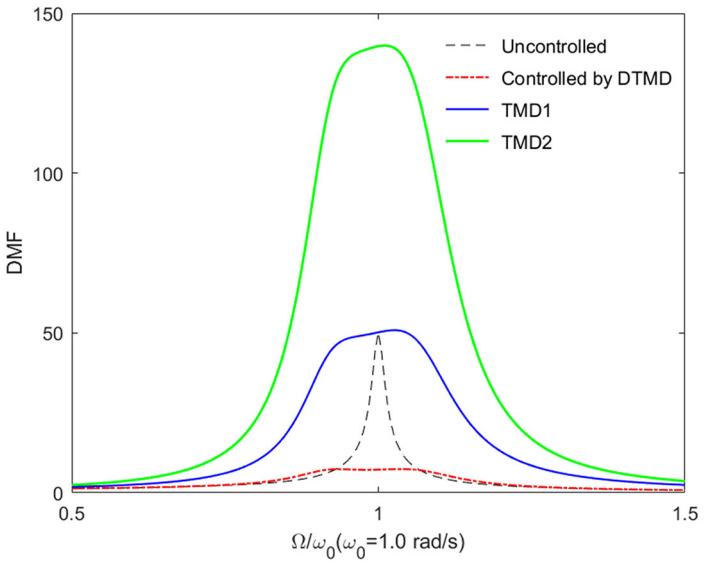

Fig. 7 DMF curves of TMD1 and TMD2 of the optimized DTMD (with μ=0.02)

5 Multi-objective optimal design

In this study, three core objectives considered for multi-objective optimal designs of DTMD are the performance, robustness and weight of DTMD. We will discuss and develop multi-objective optimization problems of DTMD in this section.

5.1 Two-objective optimization of DTMD

DTMD is a damping device added to the main structure to reduce structural vibrations. Due to the safety of the primary structure, the weight of DTMD (or the mass ratio μ) needs to be restricted. If the mass ratio is firstly chosen to satisfy required standards of design, the remaining two important targets including the effectiveness and robustness of DTMD will be considered. The aim of this optimization problem is to maximize both the vibration absorption capacity and the robustness of DTMD.

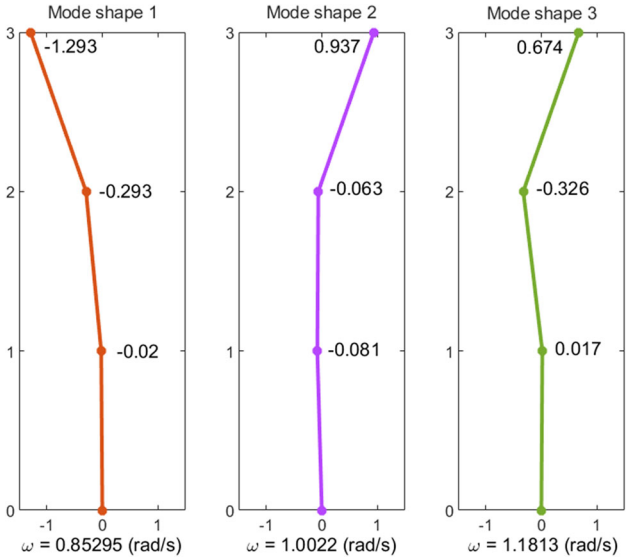

Fig. 8 Mode shapes of the DTMD-structure system

(a) Establishing objective functions

In this study, the effectiveness of DTMD is evaluated through either the target value of $\mathrm{DMF_{max}}$ or the $\mathrm{DMF_{max}}$ reduction. Here, the target value of $\mathrm{DMF_{max}}$ and the $\mathrm{DMF_{max}}$ reduction are denoted by $(\mathrm{DMF_{max}})^{\mathrm{target}}$ and ψ (%), respectively. The $\mathrm{DMF_{max}}$ reduction can be calculated by

$$\psi = \frac{(\mathrm{DMF_{max}})^{\mathrm{uncontrolled}} - (\mathrm{DMF_{max}})^{\mathrm{with\ DTMD}}}{(\mathrm{DMF_{max}})^{\mathrm{uncontrolled}}} 100\% \tag{17}$$

The value of $(\mathrm{DMF_{max}})^{\mathrm{uncontrolled}}$ is 50.0 as reported in the previous section. Hence, corresponding to each $\mathrm{DMF_{max}}$ reduction (ψ%) given, the target value of $\mathrm{DMF_{max}}$ will be determined by Eq. (17). Thus, the objective function for the effectiveness of DTMD is described as follows:

$$\mathrm{Obj\_effectiveness} : \{\mathrm{DMF_{max}} - (\mathrm{DMF_{max}})^{\mathrm{target}}\} \rightarrow \mathbf{min} \tag{18}$$

On the other hand, the robustness of the absorber is evaluated by the changing domain of the structural stiffness $[-\chi_1\%, +\chi_2\%]$. From Fig. 6, there is difference between two branches of the DMF_{max} curve. Thus, the values of χ_1 and χ_2 will be different, however, the difference can be not much. For the sake of simplicity and reduce variables in the objective function, let us assume that $\chi_1 = \chi_2 = \chi$. This means that the DTMD still maintains the similar level of efficiency (or better), while the structural stiffness is varied from $-\chi\%$ to $+\chi\%$. It is noted that the damper which gives the larger value of $\chi\%$ is more robust. In the range of $[-\chi\%, +\chi\%]$, the bottom of the DMF_{max} curve will be quite flat because all of points on this range will approach to the value of $(DMF_{max})^{target}$. The objective function for the robustness of DTMD can be established as follows:

$$\mathrm{Obj\_robustness} : \sum_{i=1}^{n} \left\{(\mathrm{DMF_{max}})^{\chi_i\%} - (\mathrm{DMF_{max}})^{\mathrm{target}}\right\}^2 \rightarrow \mathbf{min} \tag{19}$$

In Eq. (19), n is the number of chosen points on the DMF_{max} curve in the domain of $[-\chi\%, +\chi\%]$. For the sake of simplicity, choosing the distance between points within $[-\chi\%, +\chi\%]$ is equal. From there, $\chi_i\%$ can be determined by

$$\chi_i\% = -\chi\% + \frac{2\chi\%}{n-1}(i-1) \tag{20}$$

By combining Eq. (18) and Eq. (19), two-objective optimization function of DTMD is given as follows:

$$\mathrm{Two\_Obj} = \begin{cases} \{\mathrm{DMF_{max}} - (\mathrm{DMF_{max}})^{\mathrm{target}}\} \rightarrow \mathbf{min} \\ \sum\limits_{i=1}^{n} \{(\mathrm{DMF_{max}})^{\chi_i\%} - (\mathrm{DMF_{max}})^{\mathrm{target}}\}^2 \rightarrow \mathbf{min} \end{cases} \tag{21}$$

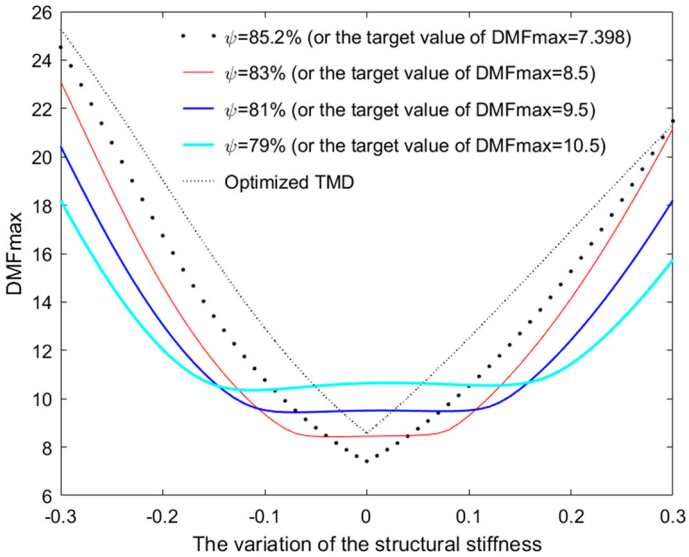

Fig. 9 DMF_{max} curve for two-objective optimal designs of DTMD (with $\mu = 0.02$)

Table 4 Optimal parameters of DTMD for two-objective optimal designs

ψ	$\text{DMF}_{\max}$	β_1	β_2	μ^{fixed}	μ_{21}	ξ_2	$\chi\%$
85.2%	7.398	1.041	0.970	0.020	0.088	0.246	0
83%	8.5	1.033	0.952	0.020	0.080	0.192	7
81%	9.5	1.044	0.941	0.020	0.099	0.205	10
79%	10.5	1.057	0.931	0.020	0.121	0.216	15

Obviously, apart from μ, μ_{21}, β_1, β_2 and ξ_2, $\chi\%$ is also a variable of the objective function Eq. (21).

(b) Numerical results

Using GAs in the Optimization Tool of MATLAB and the two-objective function in Eq. (21), Fig. 9 presents the $\text{DMF}_{\max}$ curves for two-objective optimal designs (both the robustness and effectiveness) of DTMD. The optimal parameters of DTMD for different cases of ψ are reported in Table 4. In the calculation, the mass ratio is fixed ($\mu = 0.02$) and the value of n is 5. As observed from Fig. 9, the effectiveness of DTMD will be decreased if one tries to enhance the robustness of DTMD. In the specific case of $\psi = 83\%$, the performance of DTMD is still better than that of the optimal TMD ($\text{DMF}_{\max} = 8.5$ of DTMD compared with 8.567 of the TMD), and the DTMD robustness against the drift of the structural stiffness is the range of $[-7\%, 7\%]$.

5.2 Three-objective optimization of DTMD

(a) Establishing objective functions

In this part, DTMD is optimized for three main objectives including the performance, robustness and weight of DTMD, in which the weight of DTMD is evaluated through the nondimensional quantity μ. Here, the mass ratio μ is considered in the range of $[1\%, 3\%]$ and $X\%$ is not exceeded to 30%. The three-objective function of DTMD is established as follows:

$$\text{Three\_Obj} = \begin{cases} \{\text{DMF}_{\max} - (\text{DMF}_{\max})^{\text{target}}\} \rightarrow \textbf{min} \\ \sum_{i=1}^{n} \{(\text{DMF}_{\max})^{\chi_i\%} - (\text{DMF}_{\max})^{\text{target}}\}^2 \rightarrow \textbf{min} \\ \mu \rightarrow \textbf{min} \end{cases} \tag{22}$$

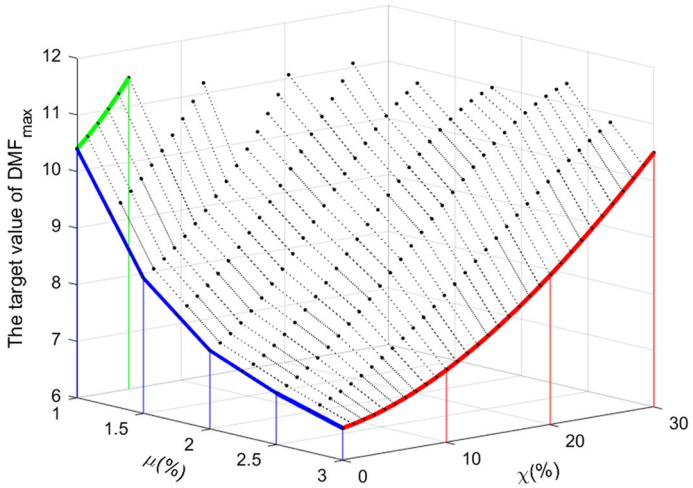

Fig. 10 Pareto optimization surface for the multi-objective optimal designs of DTMD

(b) Numerical results

It is noted that finding solutions of a three-objective optimization problem is a challenge. Thus, a suitable approach is to use two-objective optimization problems (as previously mentioned) with different values of μ. In this manner, the Pareto fronts are constituted from many two-objective optimal designs. In particular, the values of μ are predetermined in turn 1%, 1.25%, 1.5%, 1.75%, 2%, 2.25%, 2.5%, 2.75% and 3%, while $\chi\%$ represented for the robustness of DTMD changes from 0 to 30%. Figure 10 shows the Pareto optimization surface of DTMD for three objectives. In this figure, the DMF_{max} curve in the YZ plane (blue line) is the Pareto set of two-objective optimization designs relating to the performance and weight of this device. Other curves located on planes which are parallel with the YZ plane (small dotted line) represent two-objective optimal designs of the performance and weight corresponding to each predetermined value of $\chi\%$. Meanwhile, the DMF_{max} curves located on planes that are parallel with the XZ plane (big dotted line), such as the red and green lines, are other Pareto sets established for the DTMD robustness and effectiveness objectives corresponding to each value of μ given. Obviously, the Pareto optimization is always constrained by a law of trade-off. This means that if one chooses to enhance this objective, other objectives cannot be improved. For example, in the case of $\mu = 3\%$ (the red line), the robustness can increase to $\chi\% = 30\%$ if the DMF_{max} reduction is accepted to drop to 79% (corresponding to $(\mathrm{DMF}_{\max})^{\mathrm{target}} = 10.5$).

6 Summary and conclusions

Controlling vibrations of high-rise buildings by a DTMD, in which the DTMD consists of an undamped TMD and a smaller TMD, was proposed in the paper. The effects of parameters on the fundamental characteristics of a DTMD were investigated numerically through minimizing the peak structural response under harmonic excitations. The effectiveness of the optimum DTMD and the its robustness to resist the change of the structural stiffness were demonstrated. The noteworthy results achieved from this study are as follows:

(a) DTMD is significantly effective if the mass ratio of DTMD (μ_{21}) chosen is in the domain of (0, 1). Furthermore, there exists a set of optimum parameters of DTMD to maximize its vibration absorption capacity.
(b) An optimized DTMD is more effective than an optimal single TMD with the same mass ratio in mitigating structural responses.
(c) DTMD with optimal parameters is not more robust than the TMD optimized for resisting the variation in the structural stiffness. However, to achieve the same level of effectiveness as an optimum TMD, an optimized DTMD with a similar weight as the TMD offers a wider range for both frequency ratio and damping ratio. In this sense, by choosing a frequency range wider than the optimal value, the DTMD is much more robust against the changes of the frequency.
(d) This study also produces a suitable method for solving multi-objective optimization problems. Moreover, the Pareto optimization surface obtained will be helpful for designers to select a set of sufficiently good parameters instead of considering the full range of every parameter.

(e) For the configuration of DTMD, using an undamped primary TMD instead of a regular TMD offers a notable advantage compared with a traditional TMD or MTMD because of its simplicity for the maintenance and installing process.

Acknowledgements This research received no specific grant from any funding agency in the public, commercial, or not-for-profit sectors.

Funding Open Access funding enabled and organized by CAUL and its Member Institutions.

Code availability All codes that support the findings of this study are available from the corresponding author upon reasonable request after the paper has been accepted.

Declarations

Conflict of interest The authors declare no conflict of interest in preparing this article.

References

1. Momtaz, A.A., Abdollahian, M.A., Farshidianfar, A.: Study of wind-induced vibrations in tall buildings with tuned mass dampers taking into account vortices effects. Int. J. Adv. Struct. Eng. **9**, 385–395 (2017)
2. Chai, W., Feng, M.Q.: Vibration control of super tall buildings subjected to wind loads. Int. J. Non-Linear Mech. **32**(4), 657–668 (1997)
3. Cao, Q.H.: Vibration control of structures by an upgraded tuned liquid column damper. J. Eng. Mech. **147**(9), 04021052 (2021)
4. Chang, C.C., Hsu, C.T.: Control performance of liquid column vibration absorbers. Eng. Struct. **20**(7), 580–586 (1998)
5. Bui, H.L., Tran, N.A., Cao, H.Q.: Active control based on hedge-algebras theory of seismic-excited buildings with upgraded tuned liquid column damper. J. Eng. Mech. **149**, 04022091 (2023)
6. Vellar, L.S., Ontiveros-Pérez, S.P., Miguel, L.F.F., Fadel Miguel, L.F.: Robust optimum design of multiple tuned mass dampers for vibration control in buildings subjected to seismic excitation. Shock and Vib. **2019**, 1–19 (2019)
7. Samali, B., Mayol, E., Kwok, K.C.S., Mack, A., Hitchcock, P.: Vibration control of the wind-excited 76-story Benchmark Building by liquid column vibration absorbers. J. Eng. Mech. **130**, 478–485 (2004)
8. Jahangiri, V., Sun, C.: Three-dimensional vibration control of offshore floating wind turbines using multiple tuned mass dampers. Ocean Eng. **206**, 107196 (2020)
9. Lin, C.-C., Ueng, J.-M., Huang, T.-C.: Seismic response reduction of irregular buildings using passive tuned mass dampers. Eng. Struct. **22**, 513–524 (1999)
10. Gao, H., Kwok, K.S.C., Samali, B.: Characteristics of multiple tuned liquid column dampers in suppressing structural vibration. Eng. Struct. **21**, 316–331 (1999)
11. Diana, G., Resta, F., Sabato, D., Tomasini, G.: Development of a methodology for damping of tall buildings motion using tuned liquid colunm damper devices. Wind Struct. **17**, 629–646 (2013)
12. Chang, C.: Mass dampers and their optimal designs for building vibration control. Eng. Struct. **21**, 454–463 (1999)
13. Zheng, Lu., Wang, D., Masri, S.F., Xilin, L.: An experimental study of vibration control of wind-excited high rise buildings using particle tuned mass dampers. Smart Struct. Syst. **18**, 93–115 (2016)
14. Ikago, K., Saito, K., Inoue, N.: Seismic control of single-degree-of-freedom structure using tuned viscous mass damper. Earthquake Eng. Struct. Dynam. **41**, 453–474 (2012)
15. Jafarabad, A., Kashani, M., Parvar, M.R.A., Golafshani, A.A.: Hybrid damping systems in offshore jacket platforms with float-over deck. J. Constr. Steel Res. **98**, 178–187 (2014)
16. Yang, J., Sun, S.S., Du, H., Li, W.H., Alici, G., Deng, H.X.: A novel magnetorheological elastomer isolator with negative changing stiffness for vibration reduction. Smart Mater. Struct. **23**, 105023 (2014)
17. Zhu, W., Rui, X., Semiactive vibration control using a magnetorheological damper and a magnetorheological elastomer based on the bouc-wen model. Shock and Vib., vol. 2014, (2014).
18. Sun, S., Yang, J., Du, H., Zhang, S.W., Yan, T., Nakano, M., Li, W.: Development of magnetorheological elastomers-based tuned mass damper for building protection from seismic events. J. Intell. Mater. Syst. Struct. **29**(8), 1777–1789 (2018)
19. Li, C., Zhu, B.: Estimating double tuned mass dampers for structures under ground acceleration using a novel optimum criterion. J. Sound Vib. **298**, 280–297 (2006)
20. Shen, B., Wang, J., Xu, W., Chen, Y., Yan, W., Huang, J., Tang, Z.: Experimental research on damping effect of double-layer tuned mass damper for high-rise structure. Shock and Vib. **2021**, 1–22 (2021)

21. Khatibinia, M., Gholami, H., Kamgar, R.: Optimal design of tuned mass dampers subjected to continuous stationary critical excitation. Int. J. Dynam. Control **6**, 1094–1104 (2018)
22. Etedali, S., Rakhshani, H.: Optimum design of tuned mass dampers using multi-objective cuckoo search for buildings under seismic excitations. Alex. Eng. J. **57**, 3205–3218 (2018)
23. Gil-Martín, L.M., Carbonell-Márquez, J.F., Hernández-Montes, E., Aschheim, M., Pasadas-Fernández, M.: Dynamic magnification factors of SDOF oscillators under harmonic loading. Appl. Math. Lett. **25**, 38–42 (2012)
24. Varadarajan, N., Nagarajaiah, S.: Wind response control of building with variable stiffness tuned mass damper using empirical mode decomposition/Hilbert transform. J. Eng. Mech. **130**, 451–458 (2004)
25. McCall, J.: Genetic algorithms for modelling and optimisation. J. Comput. Appl. Math. **184**, 205–222 (2005)
26. Ahadi, P., Mohebbi, M. and Shakeri, K.: Using optimal multiple tuned liquid column dampers for mitigating the seismic response of structures. ISRN Civil Eng., vol. 2012, p. Article ID 592181, (2012)
27. Wu, Q., Zhao, W., Zhu, W., Zheng, R., Zhao, X.: A tuned mass damper with nonlinear magnetic force for vibration suppression with wide frequency range of offshore platform under earthquake loads. Shock and Vib. **2018**, 1–18 (2018)
28. Xue, Q., Zhang, J., He, J. and Zhang, C.: Control performance and robustness of pounding tuned mass damper for vibration reduction in sdof structure. Shock and Vib., 2016, p. Article ID 8021690, (2016)
29. Yamaguchi, H., Harnpornchai, N.: Fundamental characteristics of multiple tuned mass dampers for suppressing harmonically forced oscillations. Earthquake Eng. Struct. Dynam. **22**, 51–62 (1993)